

Multilayered Adsorption of Commensal Microflora on Implant Surfaces: an Unconventional and Innovative Method to Prevent Bacterial Infections Associated with Biomaterials

Muhammad Imran Rahim,* Katharina Doll, Nico S. Stumpp, Michael Eisenburger, and Meike Stiesch

Biomaterials may be colonized with infectious biofilms and this frequently leads to progressive loss of tissue. Bacteria encased within biofilms resist antibiotics and the host immune system. With life-threatening complications and the antibiotic resistance crisis, novel therapeutic approaches are essentially required to treat biofilm infections. Commensal microflora—particularly streptococci—modulate the immune system's ability to protect from pathogens. In imitation of this natural phenomenon, the present study describes a novel method of applying the commensal, *Streptococcus oralis*, as a coating on implants to prevent infectious biofilms. Implants are coated with a simple thermal process to circumvent sepsis persuaded by live microflora and for a stable multilayered coating. Titanium discs coated with *S. oralis* antagonize the biofilm-making capabilities of single, dual, or multispecies periodontal pathogens: *Porphyromonas gingivalis*, *Treponema denticola*, *Veillonella dispar*, and *Actinomyces naeslundii*—under both static and flow conditions. The bacterial adhesion force measured with atomic force microscopy (AFM) reduces on coated titanium suggesting that electrostatic interactions are mainly responsible for the decrease in maximum adhesion peak. Importantly, *S. oralis* coated implants are compatible with human gingival fibroblasts. *S. oralis* coating may provide a potent novel approach to prevent potentially fatal biofilm infections on biomaterials.

1. Introduction

Most dental implants consist of titanium and face constant interactions with the oral microflora, comprising more than 700 different bacterial species.^[1] They are therefore under continuous threat of bacterial invasion.^[2] Colonization of infec-

tious bacteria around dental implants may lead to the formation of biofilms,^[3] which can cause mucosal inflammation, which is associated with peri-implant bone loss and peri-implantitis.^[4] The ongoing tissue damage and bone resorption hinder the integration of the implant into tissue. Moreover, biofilms exhibit strong antibiotic resistance and are therefore impervious to therapy.^[5] Biofilm formation is a stepwise process starting from the initial bacterial adhesion, followed by microcolony formation and finally maturation into extracellular encased mature biofilms.^[6] Initial bacterial adhesion is the most critical step in biofilm formation and strategies targeting the inhibition of bacterial adhesion may be of therapeutic value.^[7] Recent progress in understanding the nature and complexity of biofilms has led to the development of antibiofilm strategies. Since antibiotics remain the “gold standard” therapeutics, local antibiotic delivery systems have been applied to implant surfaces to prevent initial bacterial adhesion.^[8] Even though most antibiotics resist bacterial attachment simply by killing the bacteria, they increase the chance that antimicrobial resistance may develop.^[9] In addition, antibiotics may kill healthy microflora and their prolonged intake will result in systemic side effects in patients.^[10] Moreover, metal ions as antimicrobial agents, such as cationic compounds, semi or fully synthetic peptides, or metallic nanoparticles (silver, copper, and zinc) have been coated on implant surfaces to prevent bacterial biofilms.^[11] These metallic nanoparticles triggered toxic effects at the implantation site, as well as systemic effects in other organs.^[12] In the context of antifouling coatings, polymeric coatings were applied on implant materials to resist bacterial adhesion and issues of severe biofilm formation.^[13] One of the critical strategies involves applying poly(ethylene glycol) (PEG) to fabricate surfaces that resist bacterial adhesion against *Escherichia coli*, *Staphylococcus epidermidis*, *Streptococcus sanguinis*, and *Lactobacillus salivarius*.^[14] However, the fabrication of polymer coating involves a complicated process and the mechanism of bacterial resistance is not universal against each bacterial species. This ineffectiveness of coating could be mainly due to the complexity of the mechanisms through which bacteria attach

M. I. Rahim, K. Doll, N. S. Stumpp, M. Eisenburger, M. Stiesch
Department of Prosthetic Dentistry and Biomedical Materials Science
Hannover Medical School
Carl-Neuberg Strasse 1
Lower Saxony Centre for Biomedical Engineering
Implant Research and Development (NIFE)
Hannover Medical School
Stadtfelddamm 34, Hannover 30625, Germany
E-mail: Rahim.Muhammad@mh-hannover.de

 The ORCID identification number(s) for the author(s) of this article can be found under <https://doi.org/10.1002/admi.202101410>.

© 2021 The Authors. Advanced Materials Interfaces published by Wiley-VCH GmbH. This is an open access article under the terms of the Creative Commons Attribution License, which permits use, distribution and reproduction in any medium, provided the original work is properly cited.

DOI: 10.1002/admi.202101410

to a surface.^[15] Moreover, polymers such as PEG undergo oxidation in media with variable compositions and can be unsuitable for long-term use.^[16] In addition, polymer coatings may cause possible side effects and complications such as hypersensitivity, secretion of toxic side products, unexpected pharmacokinetics, antagonism arising from the degradation of polymer, nonbiodegradability, and prolonged accumulation in the body.^[17]

Therefore, recent therapeutic research has concentrated on the strategy of inhibiting pathogen growth by applying healthy commensal microflora. Healthy oral microflora—particularly *Streptococcus salivarius* and *Streptococcus pyogenes*—may act as “probiotics” in the treatment of various infections of the pharyngeal mucosa, as they are living microorganisms that promote health if consumed in specific amounts.^[18] A probiotic study with *Streptococcus oralis*, *Streptococcus uberis*, and *Streptococcus rattus* found efficacious responses against infectious *Prevotella intermedia*.^[19] Regular intake of probiotic lactobacilli and bifidobacteria decreased the number of cariogenic and plaque-forming bacteria.^[20] Bacteriocins produced from *Streptococcus salivarius* were used to treat plaque (oral biofilm) in children and were found to be novel antimicrobial agents.^[21] The use of probiotic *Bifidobacterium* effectively reduced the levels of carries-associated bacteria in saliva of children.^[22] Exopolysaccharide (EPS) extracted from *Lactobacillus plantarum* effectively inhibited the formation of biofilms of *Staphylococcus aureus*, *Listeria monocytogenes*, *Pseudomonas aeruginosa*, and *Salmonella typhimurium*.^[23]

Not only living commensal microflora, but also heat killed *Lactobacillus* species exhibited effective antibacterial properties against oral pathogens that form biofilms.^[24] Moreover, artificial biofilms of the probiotic *Lactobacillus casei* on titanium increased osseointegration and prevented infections of methicillin-resistant *Staphylococcus aureus* (MRSA).^[25] However, to the best of our knowledge, there have been no studies on the use of commensal microflora to prevent implant-associated biofilm infections. In the present study, we hypothesized that commensal oral streptococci fixed as a stable coating on implant surfaces might prevent the formation of biofilms of infectious bacteria. In order to address this question, *Streptococcus oralis* was heat-coated on titanium surfaces and the anti-biofilm properties were tested against diverse periodontal pathogens under two different environmental conditions. The mechanism underlying the anti-biofilm activities of *S. oralis* coatings was investigated with single-cell force spectroscopy. *S. oralis* coated implants were also examined for cytocompatibility with human gingival fibroblasts.

2. Results

2.1. Immobilization of Commensal *S. oralis* as a Versatile Process for Coating Implant Surfaces

As the geometry of (dental) implants is often complex, any coating procedure must be as versatile as possible. For this purpose, *S. oralis* was cultured overnight and immobilized on titanium surfaces through simple heat coating procedures. In the first procedure, discs were placed directly on a hot plate

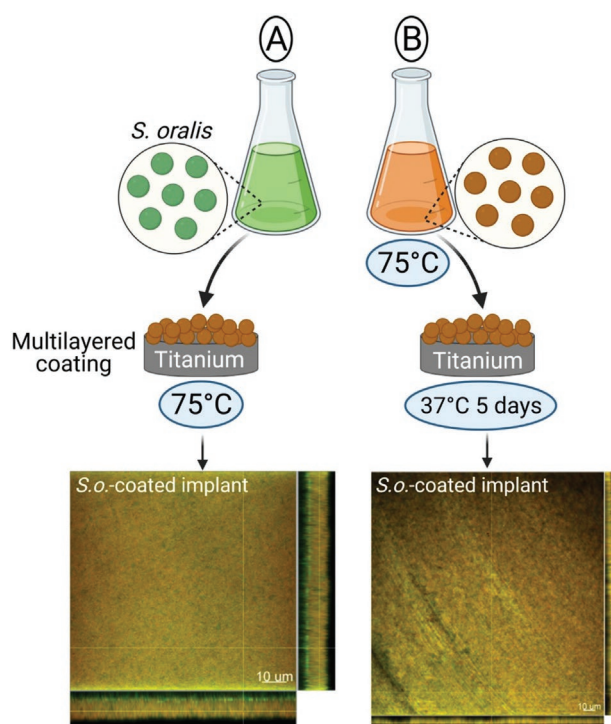


Figure 1. Schematic representation of coating procedures. Two methods were pursued to coat *S. oralis* on titanium implants. A) *S. oralis* cultures were added as thin layers (50 μ L each) on titanium discs placed directly on a hot plate adjusted to 75 $^{\circ}$ C, and a multilayered coating developed. B) *S. oralis* cultures were killed at 75 $^{\circ}$ C, and then titanium was incubated with these cultures at 37 $^{\circ}$ C for 5 d resulting in the formation of the coating.

adjusted to 75 $^{\circ}$ C and then bacterial cultures were added in layers (50 μ L). The resulting multilayered bacterial adsorption resulted in the deposition of a stable coat (Figure 1A). The second procedure was mainly established for heat-sensitive materials. Even though this is not important for dental implants, this might be necessary, e.g., for shape memory materials used for cochlear implants. In this procedure, *S. oralis* cultures were first heat killed at 75 $^{\circ}$ C and then added to implants, followed by incubation at 37 $^{\circ}$ C for 5 d (Figure 1B). This incubation resulted in slow evaporation, which allowed gradual accumulation of bacteria as coats. In summary, the proposed simple coating strategies were successful and would most probably be applicable to any desired geometry.

2.2. Stability Analysis of *S. o.*-Coated Titanium

To verify the stability of freshly coated titanium implants under physiological conditions, coated implants were incubated in cell culture medium for 48 h under standard cell culture conditions. Before immersion and incubation, the macroscopic appearance of freshly coated titanium clearly showed the accumulation of coating (Figure 2 upper part, *S. o.*-coated). After immersion of 48 h in cell culture medium, the coating resisted direct exposure to the liquid medium and was still visible on the implant surfaces (Figure 2 upper part, *S. o.*-coated (48 h)). A detailed

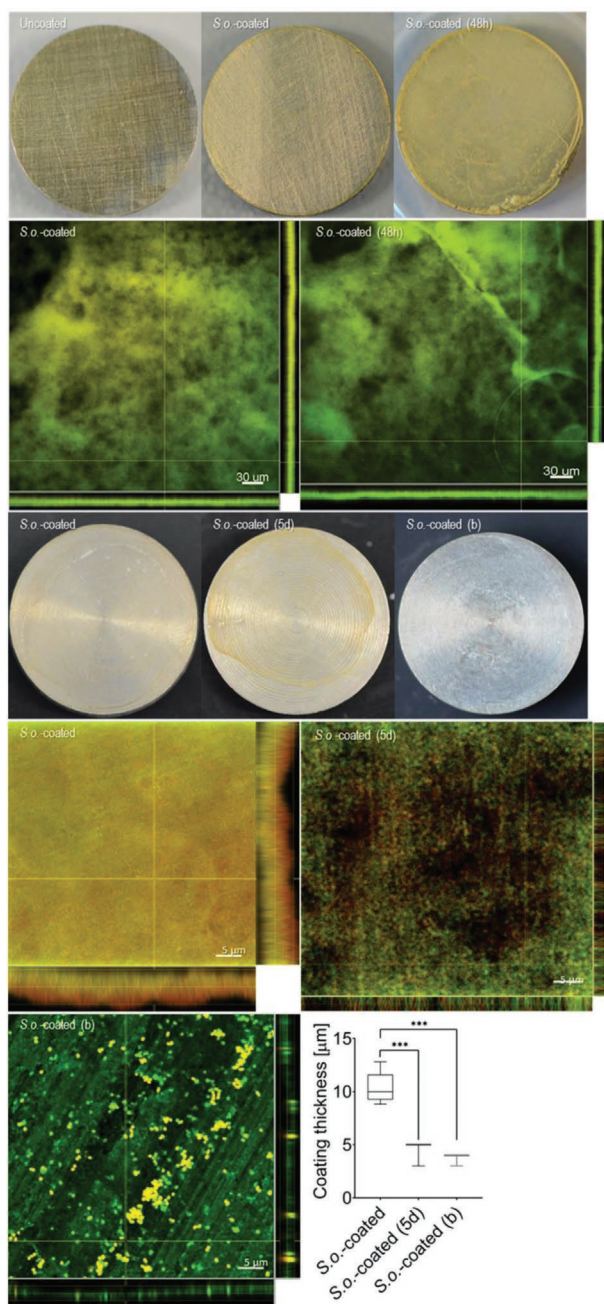


Figure 2. Macroscopic and CLSM images of uncoated and coated titanium. Upper part: titanium implants without coating (uncoated), after *S. oralis* coating (*S. o.*-coated), and coated implants after 48 h of immersion in cell culture medium (DMEM) (*S. o.*-coated (48 h)). Lower part: CLSM images of coated titanium before (*S. o.*-coated) and after 48 h of immersion in cell culture medium (*S. o.*-coated (48 h)). The yellow/orange color indicates dead bacteria. Macroscopic and CLSM images of *S. oralis* coated implants (*S.o.*-coated), *S. oralis* coated implants after 5 d of shaking at 300 rpm (*S. o.*-coated (5 d)), *S. oralis* coated implants after shaking and brushing (*S. o.*-coated (b)). Coating thickness measured on *S. o.*-coated implants, *S. o.*-coated implants after 5 d of constant shaking and *S. o.*-coated implants after 20 times of brushing.*** $p < 0.0005$.

analysis of the coating layer by confocal microscopy further confirmed that—even after direct exposure to physiological liquid medium—the densely packed coating layer was clearly

visible. The thickness of the coat on titanium was similar before and after 48 h of incubation (Figure 2 lower part, *S. o.*-coated and *S.o.*-coated (48 h)). The stability testing of the coating after a constant shaking speed of 300 rpm for five days showed morphologically visible coating, which was seemingly less thick than fresh coating (Figure 2, *S. o.*-coated (5d)). Coating subjected to 20 times of mechanical brushing after 6 h of shaking at a speed of 300 rpm indicated a weak coating layer still visible on implant surfaces (Figure 2, *S. o.*-coated (b)). The microscopic thickness of coating from the fresh coating ($10.37 \mu\text{m} \pm 1.37$) had significantly decreased on implants ($4.75 \mu\text{m} \pm 0.70$) after five days of shaking at 300 rpm or brushing ($4.5 \mu\text{m} \pm 1.30$) (Figure 2, *S.o.*-coated, *S.o.*-coated (5d) and *S.o.*-coated (b)). This experiment confirmed freshly coated implants were initially stable under static or mobile physiological conditions, which is an essential prerequisite for further in vivo implantation.

2.3. Coatings Resist the Biofilms of Commensals and Periodontal Pathogens

To investigate whether *S. oralis* coatings resist the adhesion of diverse bacterial species, three different periodontal pathogens comprising; *S. oralis*, *Veillonella dispar*, *Porphyromonas gingivalis*, and *Treponema denticola* were cultured on *S. oralis* coated implants. The capacity of each bacterium to form biofilms was investigated by LIVE/DEAD staining followed by confocal microscopy. Uncoated titanium showed high expression of green fluorescence, which was indicative for viable biofilms were formed by (Figure 3 left column). There was no accumulation of green fluorescence representative for growth of viable biofilms around *S. o.*-coated implants (Figure 3 right column). Instead, only a yellow/orange layer of densely packed, dead coated bacteria was visible. According to these results, followed by *S. oralis* coating, implants clearly prevented initial colonization of commensal as well as infectious bacteria and subsequent biofilm formation (Figure 3 right column).

Since the coating mass was composed of heat killed streptococci, it was considered that LIVE/DEAD staining and confocal microscopy would probably not visualize biofilms adequately. Therefore, *S. o.*-coated and uncoated titanium was incubated with the most infectious biofilm-forming species, *P. gingivalis* and *T. denticola*, for 48 h and then observed with scanning electron microscopy (SEM). Homogenous *P. gingivalis* biofilm growth was present on uncoated titanium surfaces (Figure 4 left and Figure S1, Supporting Information white arrows). Few *P. gingivalis* cells were visible on the surface of *S. o.*-coated titanium (Figure 4 *S. o.*-coated and Figure S1, Supporting Information represented by white arrows). At higher magnifications, few detectable *P. gingivalis* could be clearly seen and differentiated from *S. oralis* coated implants (Figure 4 and Figure S1, Supporting Information). *T. denticola* exhibited huge biofilm formation on uncoated titanium surfaces (Figure 4 white arrow and Figure S1, Supporting Information white arrows). *S. o.*-coated titanium drastically reduced biofilm formation by *T. denticola* as well (Figure 4 right column and Figure S1, Supporting Information represented by white arrows). These results confirm the results of confocal microscopy analyses and demonstrate that *S. oralis* coats greatly impair the development of biofilms on titanium.

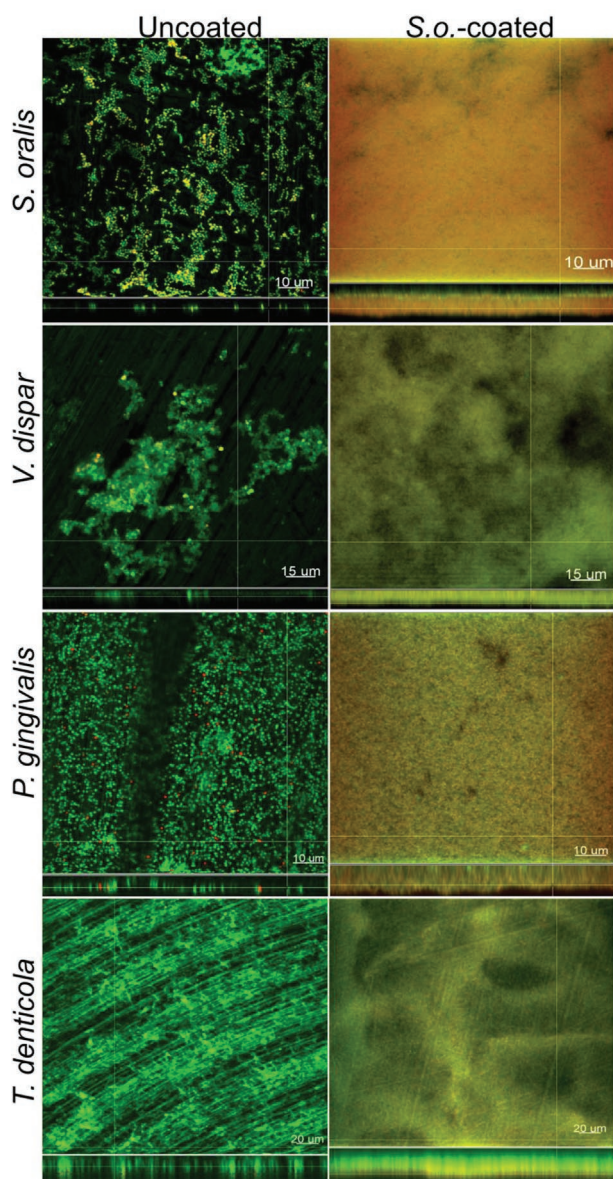


Figure 3. *S. oralis* coated implants antagonize the growth of bacterial biofilms. Typical CLSM images (top view and cross section) of biofilm growth on uncoated titanium surfaces, as indicated by green fluorescence of *S. oralis*, *V. dispar*, *P. gingivalis*, and *T. denticola* (left side, top to bottom). *S. o.*-coated titanium surfaces completely inhibit biofilms from the same pathogens (right side, top to bottom).

2.4. *S. oralis* Coated Implants Are Resistant to the Formation of Multispecies Biofilms

Dental implant infections in clinical situations involve a consortium of diverse bacterial species, in the presence of constantly flowing oral saliva. Therefore, layer-wise coated implants were allowed to interact with multispecies oral biofilms comprising; *S. oralis*, *V. dispar*, *Actinomyces naeslundii*, and *P. gingivalis*. The experiment was performed in an oral flow chamber system, that mimicked the flow of oral saliva. Biofilm formation was then evaluated by LIVE/DEAD

fluorescence staining and CLSM, whereas the presence of all species—at least in the control biofilm—was verified by fluorescence in situ hybridization (FISH). This multispecies biofilm on uncoated titanium was dominated by *S. oralis* (blue), followed by *V. dispar* (yellow), *A. naeslundii* (green), and *P. gingivalis* (red) (Figure 5 Multispecies biofilms). The uncoated titanium allowed the formation of multispecies biofilms and displayed higher surface coverage of $48.05\% \pm 16.71$ (Figure 5 uncoated). *S. o.*-coated implant surfaces clearly reduced the formation of multispecies biofilms and bacterial surface coverage of $2.68\% \pm 0.93$ (Figure 5 *S. o.*-coated). These results exhibit additional valuable aspects of *S. oralis* coats, as they inhibit both single and multispecies bacterial biofilms under flowing conditions.

2.5. An Alternative Method of Coating *S. oralis* on Titanium Maintains the Prevention Bacterial Biofilms

To optimize streptococcus coatings for heat-sensitive materials, a second coating procedure was investigated, that employed previously heat killed bacteria. In this method, *S. oralis* was first killed at 75°C and then cultured on titanium discs for 5 d at 37°C . This method caused slow evaporation and gradual accumulation of *S. oralis* on titanium and coating mass became visible on implant surfaces (Figure 6 right side). To investigate anti-biofilm properties, coated implants were likewise incubated with *P. gingivalis* and *T. denticola* for 48 h. Biofilms from *P. gingivalis* or *T. denticola* were visible on uncoated titanium surfaces using LIVE/DEAD staining and CLSM (Figure 6 left side, top to bottom). *S. o.*-coated implant surfaces, in contrast, maintained resistance to *P. gingivalis* and *T. denticola* biofilms. As an additional step in the analysis of coated implants, both uncoated and *S. o.*-coated titanium were subjected to dual-species biofilms comprising mixture of *P. gingivalis* and *T. denticola* (Figure 6 right side, top to bottom). The coated implants maintained resistance and inhibited the colonization of even dual-species biofilms. These findings confirm that streptococcus coatings applied by either procedure repel the biofilms of infectious bacteria as single or dual-species.

2.6. Antibiofilm Properties Are Specific for *S. oralis* Coatings

To investigate whether the biofilm repellent properties were peculiar to *S. oralis*, or whether other streptococci could exhibit similar effects, *S. salivarius* was coated on titanium discs through the heat mediation process. To see potential synergistic effects, *S. salivarius* and *S. oralis* were mixed and coated on titanium. The resulting coatings were treated with *P. gingivalis* to form biofilms. After 48 h of incubation, *P. gingivalis* biofilms were visible on uncoated titanium samples (Figure 7 uncoated and S2, Supporting Information). As previously described, *S. oralis* coatings were resistant and inhibited the growth of *P. gingivalis* biofilms (Figure 7 *S. o.*-coated). In contrast, *S. salivarius* coatings could not resist biofilm formation by *P. gingivalis* (Figure 7 *S. s.*-coated and Figure S2, Supporting Information). This was most probably due to the fragility of

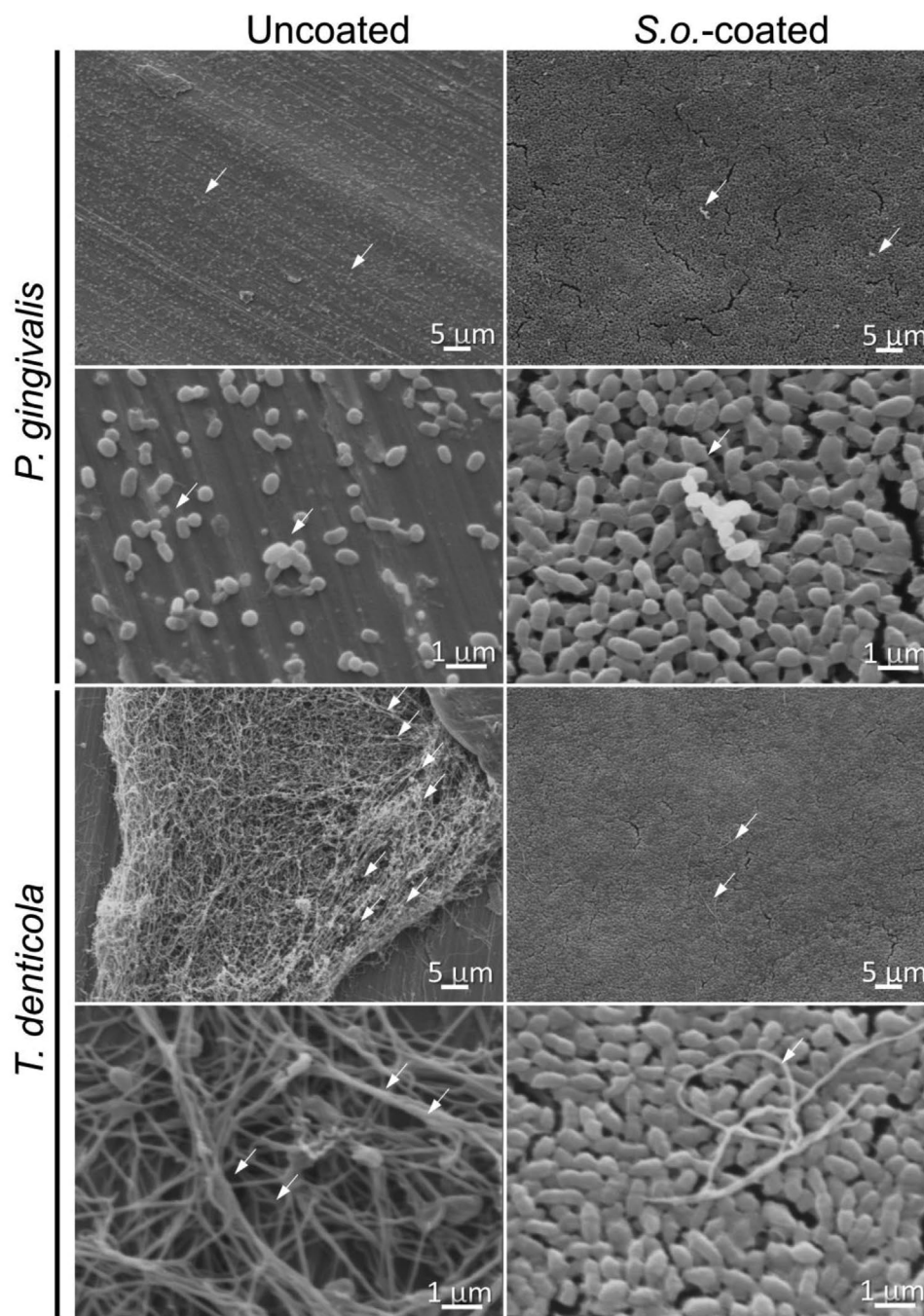


Figure 4. Typical SEM images of biofilm growth. Uncoated titanium discs are susceptible to the growth of infectious *P. gingivalis* and *T. denticola* biofilms (left column, top to bottom). *S.o.*-coated titanium exhibits strong resistance toward the colonization of infectious biofilms (right column, top to bottom). White arrows indicate only *P. gingivalis* and *T. denticola* grown on uncoated and on *S.o.*-coated titanium.

this coating—it mainly became detached and only some coated spots remained. A similar but weaker effect was observed from mixed coatings of *S. oralis* and *S. salivarius*. They also appeared fragile and some areas were already detached from the surfaces (Figure 7 *S. o.-S.s.*-coated, white arrows). On these empty surfaces, *P. gingivalis* biofilms were visible (Figure 7 *S. o.-S.s.*-coated, white arrows). To analyze the effect of *S. oralis* coatings

more closely, titanium discs were prepared that were only partially coated. *P. gingivalis* cultured on these discs clearly discriminated coated from uncoated areas, as only on the latter could biofilm formation be observed (Figure 7 *S. o.*-coated and Figure S2, Supporting Information). These findings indicate that biofilm repellent properties were specific for the coating with *S. oralis*.

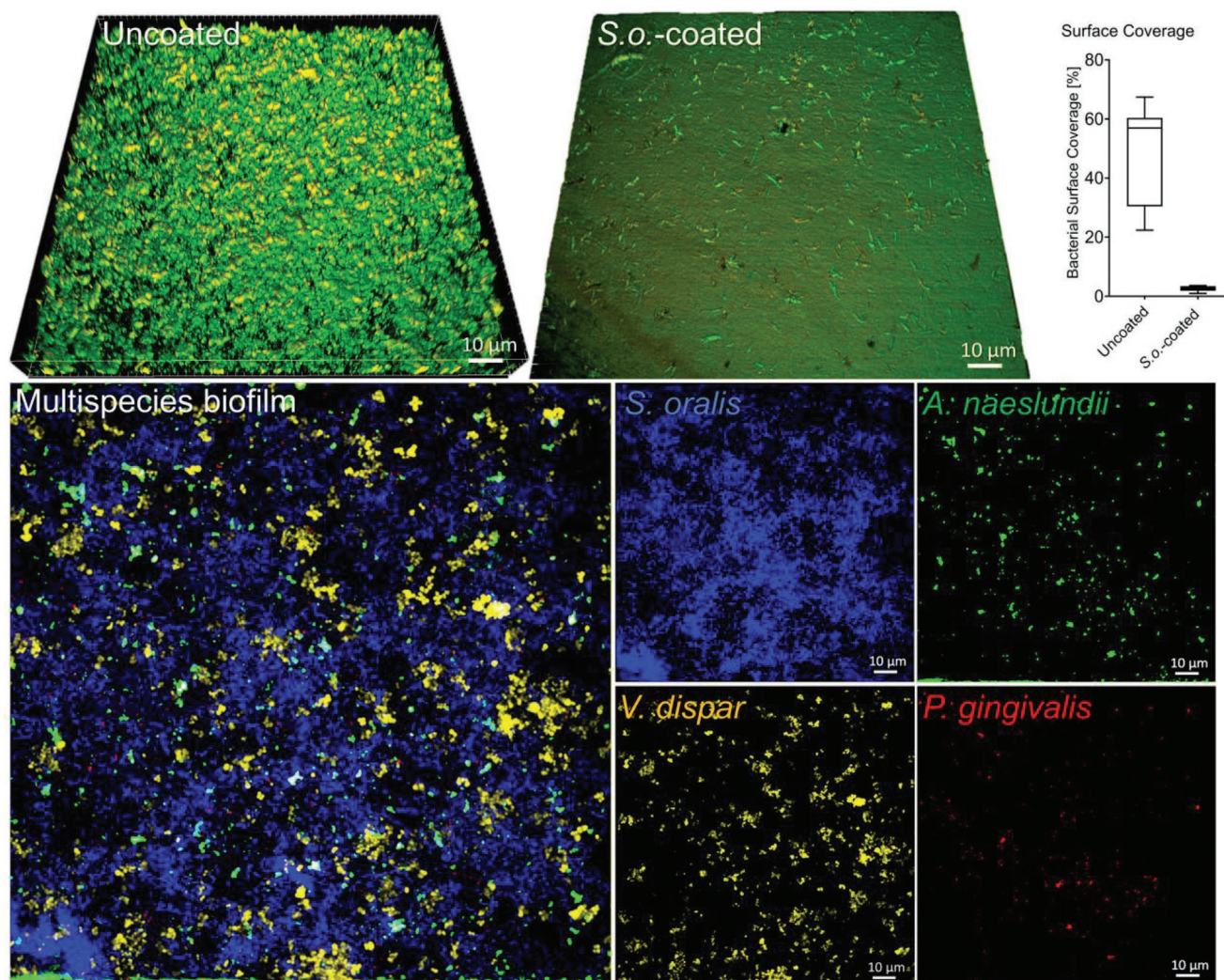


Figure 5. *S. o.*-coated titanium implants resist multispecies biofilms in a flow chamber system. 3D-reconstruction of LIVE/DEAD stained multispecies biofilm growing on uncoated titanium (uncoated) and *S.o.*-coated titanium that was resistant to multispecies biofilm (*S. o.*-coated). Box plots of bacterial surface coverage quantified from uncoated and *S.o.*-coated titanium (bacterial surface coverage). FISH staining of multispecies biofilm (multispecies biofilm) from uncoated implant showing four different bacterial species on the right side as; *S. oralis*, *A. naeslundii*, *V. dispar*, and *P. gingivalis*.

2.7. Less-Adhesive Properties of *S. o.*-Coated Titanium

These results indicate that *S. oralis* coats repel biofilms by reducing adhesion. To investigate this hypothesis, the bacterial adhesion forces of *S. oralis* and *P. gingivalis* on *S. o.*-coated and uncoated titanium surfaces were directly measured by means of single-cell force spectroscopy. Typical force–distance curves clearly showed that *S. oralis* coats reduced the maximum adhesion force (deepest point of force–distance curve) compared to uncoated titanium surfaces (Figure 8A). Quantification revealed that bacterial adhesion forces were lower on coated titanium surfaces than on uncoated surfaces (Figure 8B). The same effect could be detected for *P. gingivalis*. Typical force–distance curves showed that the *P. gingivalis* adhesion force was less on *S. o.*-coated titanium surfaces than on uncoated titanium controls (Figure 8C). Quantification of the results confirmed this difference (Figure 8D). These results verified that the developed *S. oralis* coats exhib-

ited less adhesive properties. It is most probable that conditions for the formation of biofilms are less favorable when the adhesion forces are lower.

2.8. Coatings Are Nontoxic for Human Gingival Fibroblasts

Before applying the proposed novel coats to humans or animals, it is obligatory to perform cell culture assays to verify that they are not toxic. For this purpose, the biocompatibility of titanium coated with *S. oralis* was investigated with human gingival fibroblasts by employing a fluorometric CellTiter-Blue assay, which measures cellular reduction capacity through resazurin color change.^[26] After 24 h of incubation, cellular metabolic activities decreased slightly on *S. oralis* coated titanium compared to uncoated titanium (Figure 9). At later time points (48 h), cellular metabolic activities in the presence of *S. o.*-coated titanium became similar to uncoated titanium

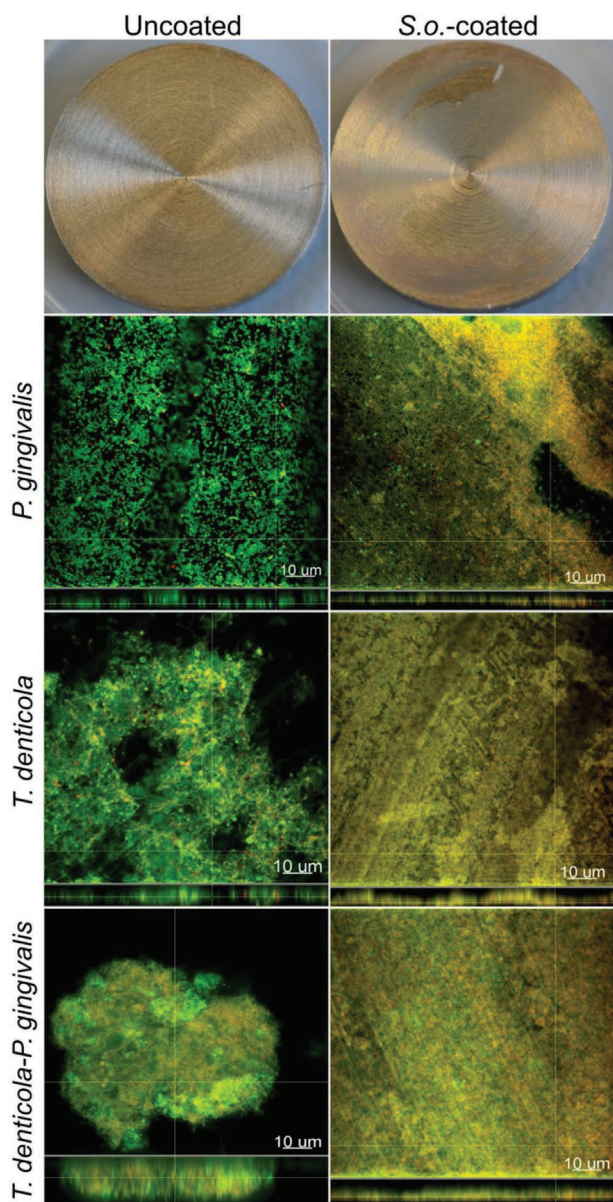


Figure 6. Typical CLSM images (top view and cross section) of titanium coated with heat killed microflora to inhibit bacterial biofilms. Uncoated implant surfaces show the accumulation of green fluorescence representative for *P. gingivalis* and *T. denticola* biofilms as single or dual species cultures by green fluorescence (left side, top to bottom). *S. o.*-coated titanium inhibits the colonization of bacterial biofilms and only shows the yellow/orange fluorescence of the dead coated bacteria (*S. o.*-coated).

(Figure 9). After 72 h of incubation, only a slight difference in metabolic activities was observed between uncoated and *S. o.*-coated implants. As monitored by scanning electron microscopy, the general morphology of human gingival fibroblasts was similar on uncoated and coated titanium (Figure 9 uncoated and *S. o.*-coated a to c). The cells density was relatively high on uncoated titanium compared to *S. o.*-coated implants (Figure 9 uncoated). Coated implant surfaces were compatible with cells; however, the growth pattern was variable on coated surfaces (Figure 9a–c). Overall, *S. oralis* coating

was not toxic and exhibited excellent properties to support the adhesion of human gingival fibroblasts. Thus, further testing of *S. oralis* coated titanium implants can be envisioned for future clinical application.

3. Discussion

Bacterial biofilms may develop on medical implants, but are intrinsically resistant to many therapeutic approaches.^[27] The underlying reason for this is that bacteria can adhere to implant surfaces and form infectious films.^[28] Therefore, novel therapeutic approaches are required to reduce initial bacterial adhesion to implant surfaces. The human oral microbiome comprises diverse bacterial species—mostly commensals—that protect host tissue from colonization by infectious pathogens.^[29] Moreover, commensal bacteria support host immunity against infectious pathogens and maintain homeostatic balance with host immune cells.^[30] After insertion, healthy dental implants are immediately colonized by commensal bacterial species, including *S. oralis*, which remains the initial predominant colonizer.^[31] Human gingival epithelial cells (HGEps) challenged with *S. oralis* biofilm showed mild transcriptional inflammatory response suggesting that they can protect tissue.^[32] Nevertheless, before medical device approval for clinical application, in vivo investigation involving implantation into bones and monitoring of local as well as systemic side effects is a prerequisite. The current study focussed on the commensal *S. oralis* as this is a major component of oral microflora, acts symbiotically with host immunity and is constantly present around oral implants or natural teeth.^[33] These findings led us to think that commensal microflora might be used as an innovative coating on implant surfaces to circumvent the initial adhesion of infectious biofilms. A simple repeated thermal process was used to establish a reliable multilayered coating of *S. oralis* on the frequently used titanium implant material. This method may easily be adapted to any implant geometry. A major issue with implant coatings remains their stability, which needs to persist under in vivo conditions for the required period of time. The novel method allowed the gradual accumulation of a coating material (microflora), which maintained their mass even after direct exposure to physiological solutions under static or continuous shaking conditions. Even though coating thickness had significantly decreased, the underlying coating layer survived even after the constant shaking process. In addition, brushing coating after 6 h of shaking could not wholly remove the coating from implant surfaces. Such robust coating stability even on implant surfaces ensures the validity of established coating methods and prolonged protection from the colonization of infectious biofilms. These results are promising for further in vivo applications that demand prolonged stability of coating during surgical procedures and later inside the host tissue. Furthermore, this coating was evaluated for a variety of bacteria as single, dual or complex multispecies biofilms under two different environmental conditions. In a static environment, the coating resisted the formation of biofilms of *S. oralis*, *V. dispar*, *P. gingivalis*, and *T. denticola*. This is of particular interest, as *S. oralis* and *V. dispar* are among the initial colonizers of

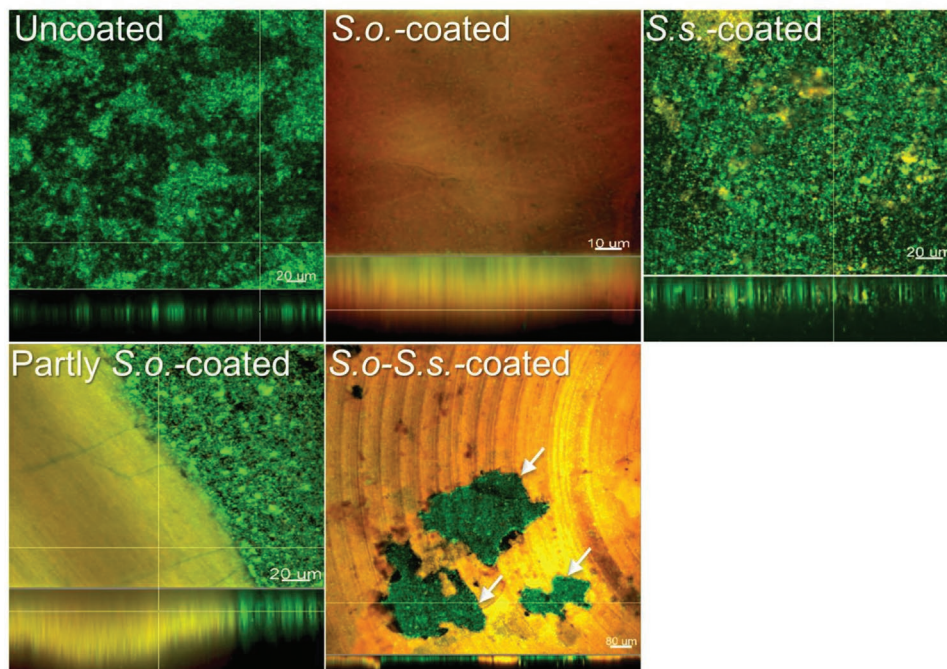


Figure 7. Sole application of *S. oralis* led to the formation of stable and biofilm repellent coats. Typical CLSM images (top view and cross section) of *P. gingivalis* biofilms (green fluorescence) on uncoated, *S. oralis* coated (*S.o.*-coated) and *S. salivarius* coated (*S.s.*-coated) titanium surfaces, as well as *P. gingivalis* grown at the interface of *S. oralis* coated or uncoated titanium (Partly *S.o.*-coated), as well as *P. gingivalis* on implants coated with mixture of *S. salivarius* and *S. oralis* (*S.o.-S.s.*-coated). The coatings are visible as yellow/orange fluorescence of dead bacteria. White arrows indicate *P. gingivalis* biofilm on exposed surfaces of detached coating.

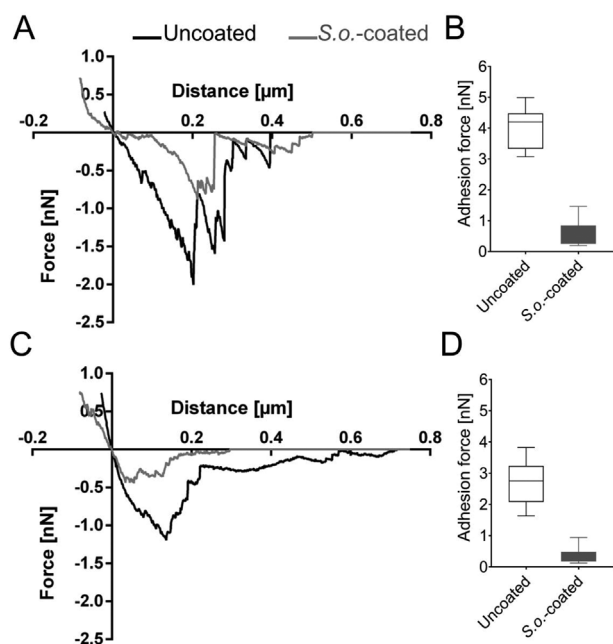


Figure 8. Antibiofilm properties of *S. oralis* coats are associated with the inhibition of bacterial adhesion. Typical force–distance curve showing A) *S. oralis* and C) *P. gingivalis* adhesion forces on *S. o.*-coated (gray) and uncoated titanium (black). Box plot of maximum adhesion force measured for B) *S. oralis* and D) *P. gingivalis* on uncoated (empty box) and *S. o.*-coated titanium (gray box).

biofilms formation in the oral cavity and thereby pave the way for biofilm formation by *P. gingivalis* and *T. denticola*. Both of these bacteria belong to the highly pathogenic “red complex” that is frequently responsible for the destruction of soft and hard tissues.^[34] The novel coating procedure therefore seems to be able to inhibit several stages of the complex development of oral biofilms. To simulate this complexity even more closely, biofilms were prepared from multiple species of oral bacteria and their interactions were studied under physiological flow conditions.^[35] Uncoated titanium allowed the establishment of multispecies biofilms and bacterial surface coverage of 48.05 ± 16.71 . Contrary to it, *S. oralis* coated implants significantly reduced the adhesion of multispecies biofilms and surface coverage by $2.68 \pm 0.93\%$. This surface coverage is less than previous findings reported for silver coating ($16.97 \pm 9.33\%$) and titanium nanotubes (8%).^[36] This indicates that coating remained stable under flowing conditions and decreased the adhesion of multispecies biofilms. The coating method was optimized for heat-sensitive materials; the bacteria were first heat killed and then conditioned as coating on the titanium surfaces. A stable coat could also be achieved with this approach. Coats resulting from this procedure likewise exhibited anti-biofilm properties against *P. gingivalis* or *T. denticola* in mono- and dual species biofilms. In the future, this process would facilitate the application of coats on heat-sensitive implant materials, like silicone, biodegradable biopolymers, and materials of biological origin and with retention of the original

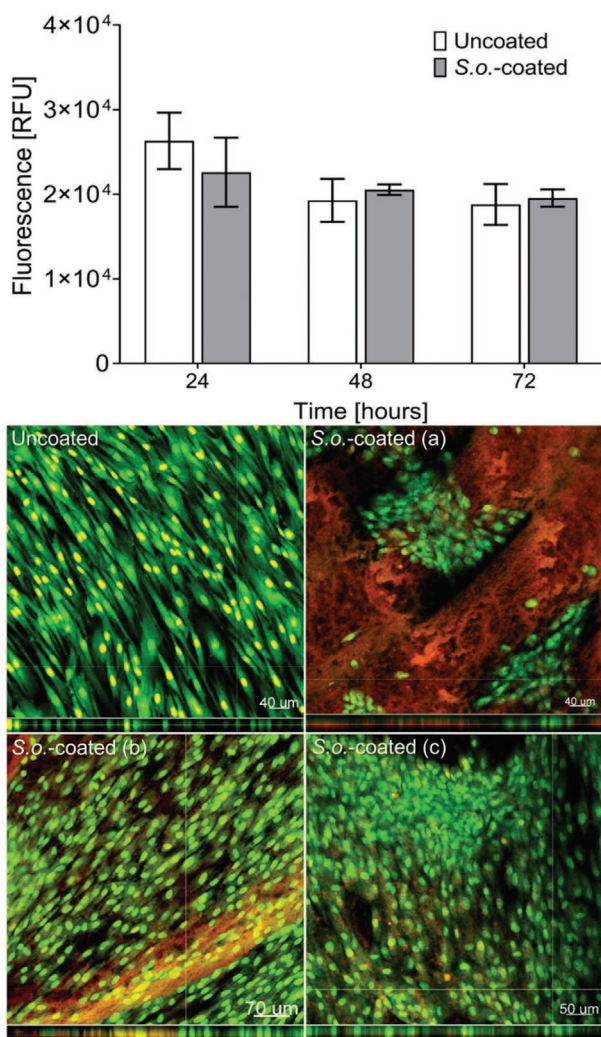


Figure 9. Biocompatibility of *S. oralis* coated titanium with human gingival fibroblasts (HGFs). Human gingival fibroblasts were seeded on *S. oralis* coated and uncoated titanium samples and metabolic activity was analyzed after 24, 48, and 72 h. Graph bars show the mean \pm standard deviation of gingival fibroblasts viability on uncoated titanium (white bars) and *S. o.*-coated titanium (gray bars) at the indicated time points. Human gingival fibroblasts on uncoated and *S. oralis* coated titanium after 72 h of cultivation (*S. o.*-coated a to c).

anti-biofilm properties.^[37] The genus *Streptococcus* comprises a wide variety of bacteria. *S. salivarius* is the first colonizer of the human oral cavity after birth, establishes immune homeostasis and regulates host inflammatory responses.^[38] A coat of *S. salivarius* regulates the corrosion of titanium.^[39] Moreover, *S. oralis* in combination with *S. salivarius* has been successfully used to treat acute otitis media.^[40] Therefore, *S. salivarius* in the *Salivarius* group was coated alone on titanium or in combination with *S. oralis*, in the *Mitis* group, through the direct thermal process. However, when these coated implants were incubated with *P. gingivalis* biofilms, the *S. salivarius* coats became fragile and unstable and the development of *P. gingivalis* biofilms could not be prevented. The implants coated with the combination of *S. salivarius* and

S. oralis were less fragile, but could not completely prevent the colonization of *P. gingivalis* biofilms. This suggests that the coats established from *S. oralis* alone were stabler and were better at preventing the development of infectious biofilms.

As all our results indicate that the *S. oralis* coat inhibited adhesion, this hypothesis was directly addressed by measuring the bacterial adhesion forces at the level of a single cell. As this process is fairly complex, measurements were only performed for *S. oralis* and *P. gingivalis*. Reduced adhesion forces were in fact observed for both species on *S. o.*-coated titanium surfaces. This means that the electrostatic interactions, which are mainly responsible for the maximum adhesion peak, were reduced on the *S. o.*-coated surfaces.^[41] Metallic titanium is highly positively charged in ionic solutions, such as buffer or medium.^[42] Thus, we would expect that the negatively charged bacterial membrane would be strongly attracted to metallic titanium. With the novel coating, this charge is most probably obscured. Even though *S. oralis* membranes may be damaged by the thermal coating process, they may be presumed to retain some negative charge. Consequently, less adhesion of infectious bacteria was expected as they are negatively charged. This mechanism could explain less adhesive properties of dead commensal coating against infectious biofilms. Although coatings are very stable and repel biofilms, novel coatings can only be used in vivo if they are compatible with the host. The coats' biocompatibility was initially tested with a basic metabolic assay for mammalian cells. This study employed human gingival fibroblasts (HGFs) since these cells are responsible for constant adaptation, regeneration, and wound healing.^[43] They effectively seal soft tissue ability and subsequently are critical in sustaining inflammation in periodontal diseases.^[44] Consequently, the healthy bioactivity of HGFs with *S. o.*-coated titanium could be of great importance in forming peri-implant soft tissue seal. It is notable that human gingival fibroblasts exhibited healthy metabolic activities when seeded on *S. o.*-coated titanium surfaces—which suggests that coated implants can significantly promote early adhesion and proliferation of HGFs and that they generate strong competition against initial bacterial attachment at implant sites. There is no literature describing the direct growth of human gingival fibroblasts on implant surfaces coated with commensal microflora. Interestingly, *S. oralis* coated implant surfaces were compatible and allowed an unrestrained proliferation of human gingival fibroblasts. It indicates that coating was non-toxic and facilitated the adhesion process of host cells. The morphology and growth pattern of human gingival fibroblasts was the same on coated and uncoated implant surfaces. Even though fibroblasts demonstrated low proliferation on regions with thick coatings, there was no significant difference in the morphology of cells. Human gingival fibroblasts are the most important cells of peri-implant mucosa.^[45] Good compatibility of human gingival fibroblasts is suggestive for further compatibility of coated implants with osteoblasts and immune cells to investigate homeostasis and immunomodulation. These findings are suggestive that coatings could be reliably tested in animal models to promote future clinical applications. The complete surgical procedure for implant placement in clinics involves several procedures and carries risks for the removal of implant coating and biofilm infection at the implant site.^[46] Therefore, the stability testing of coated implants after

placement into bones of animal models is essentially a required step. If the coating seems fragile to maintain required stability inside bones, this study has shown stability of coating at shaking speed of 300 rpm, which suggests the persistence of coating on abutment within the soft tissue above peri-implant bone level. The prolonged protection of coated abutment within periimplant soft tissue is essential since these regions remain the initial surfaces for the colonization of bacterial biofilms.

4. Conclusion

This study presents an innovative strategy to protect implant surfaces from infectious biofilms by the oral commensal *S. oralis*. A simple thermal process was developed for the accumulation of stable multilayered coating of commensal *S. oralis* on titanium surfaces. The coating remained stable and maintained thickness against exposure to cell culture medium under static and mobile conditions. The coated titanium circumvented the adhesion of diverse bacterial species—either alone or in combination as multispecies biofilms under both static and flow conditions. This suggests that novel implant coating has the potential to prevent life-threatening implant-associated infections for dental implants and for other organs. Since the coating from commensal microflora was nontoxic and compatible with human gingival fibroblasts, future in vivo investigations can be designed to promote the desired clinical application.

5. Experimental Section

Growth and Cultivation of Bacteria: *Streptococcus oralis* (ATCC 9811, American Type Culture Collection, Manassas, USA), *Streptococcus salivarius* (DSM 20067, German Collection of Microorganisms and Cell Cultures, Braunschweig, Germany), *Actinomyces naeslundii* (DSM 43013), *Veillonella dispar* (DSM 20735), *Porphyromonas gingivalis* (DSM 20709), and *Treponema denticola* (DSM 14 222) were routinely stored as glycerol stocks at -80°C . *S. oralis* and *S. salivarius* were grown overnight at 37°C under aerobic conditions in Tryptone Soy Broth (TSB, Oxoid Limited, Hampshire, UK), supplemented with 10% yeast extract (Carl Roth GmbH + Co. KG, Karlsruhe, Germany). *A. naeslundii*, *V. dispar*, and *P. gingivalis* were cultured for 48 h on fastidious anaerobe agar plates (LabM, Heywood, UK), supplemented with 5% sheep blood at 37°C under anaerobic conditions (80% N_2 , 10% H_2 , 10% CO_2). Small colonies of *A. naeslundii* or *P. gingivalis* were inoculated overnight in Brain Heart Infusion medium (BHI; Oxoid Limited), supplemented with $10\ \mu\text{g mL}^{-1}$ vitamin K (Carl Roth GmbH + Co. KG) under anaerobic conditions. *T. denticola* was cultured at 37°C under anaerobic conditions in new oral spirochete medium (NOS, Oxoid Limited) medium for 72 h.^[47]

Coating Procedures: Overnight cultures of *S. oralis* were adjusted to an optical density at 600 nm of $\text{OD}_{600} = 1.5$ and centrifuged at $4000 \times g$ for 15 min. After centrifugation, the supernatant was discarded and the bacterial pellet was suspended in Milli-Q. The procedure was repeated and then the suspension was used for coating. In the first coating method, titanium discs of 12 mm diameter and 3 mm thickness were placed on a hot plate heated to 75°C . Each titanium disc was wetted with $50\ \mu\text{L}$ of the bacterial culture, liquid was allowed to evaporate and the process was repeated until a total bacterial volume of 1 mL ($\text{OD}_{600} = 1.5$) was conditioned as a multilayered coating on each surface. During the coating procedure, the bacterial suspension was regularly vortexed. In the second coating procedure, *S. oralis* ($\text{OD}_{600} = 1.5$) were first heat killed for 15 min at 75°C and the titanium discs were then directly incubated with these heat killed microflora at 37°C for 5 d (1 mL per disc). For

S. salivarius coatings, *S. salivarius* were adjusted to $\text{OD}_{600} = 1.5$ in Milli-Q and $50\ \mu\text{L}$ of bacterial culture was added on titanium discs placed on a hot plate. The process was repeated unless 1 mL of total bacterial culture was coated on each surface. Coats from mixed *S. oralis* and *S. salivarius* cultures were prepared by mixing $500\ \mu\text{L}$ from each bacterium ($\text{OD}_{600} = 1.5$). $50\ \mu\text{L}$ from this mixed culture was added to titanium discs placed on a hot plate and allowed to evaporate until a multilayered coat on titanium surface was prepared from 1 mL per disc.

Stability Testing of Coated Implants: *S. oralis* coated implants cultured in Dulbecco's modified Eagle medium (Biochrom AG, Berlin, Germany), supplemented with 10% fetal bovine serum (PAN-BIOTECH GmbH, Aidenbach, Germany), $100\ \text{U mL}^{-1}$ penicillin, and $100\ \mu\text{g mL}^{-1}$ streptomycin (Biochrom AG, Berlin, Germany) were incubated under constant shaking at speed of 300 rpm at 37°C for 5 d. Coated implants incubated for 6 h in cell culture medium at constant shaking of 300 RPM at 37° were brushed 20 times ($N = 8$). These implants were stained with Syto9 and propidium iodide and imaged macroscopically or by confocal laser-scanning microscopy (CLSM, Leica TCS SP2, Leica Microsystems, Mannheim, Germany). Thickness of coating was further measured with the Imaris (8.2) software package (Bitplane AG, Zurich, Switzerland). The difference in coating thickness was evaluated by the Mann-Whitney test. Values of $p < 0.05$ were considered statistically significant. Statistical analyses were performed using GraphPad Prism software 8.0 (GraphPad Prism Software Inc., La Jolla, USA).

In Vitro Biofilm Assays: In vitro biofilm assays were performed on both coated and uncoated titanium discs (each type in triplicates) by *S. oralis*, *V. dispar*, *P. gingivalis*, or *T. denticola* ($N = 8$). Discs exposed to *S. oralis* ($\text{OD}_{600} = 0.05$ in TSB + 10% yeast extract and $50 \times 10^{-3}\ \text{M}$ glucose, Carl Roth GmbH + Co. KG, Karlsruhe, Germany) were incubated for 48 h at 37°C in the presence of 5% CO_2 . Incubations with *V. dispar* or *P. gingivalis* ($\text{OD}_{600} = 0.05$) cultures were performed in BHI supplemented with vitamin K at 37°C under anaerobic conditions. Incubation with *T. denticola* ($\text{OD}_{600} = 0.05$) was performed in NOS medium at 37°C under anaerobic conditions. Incubations with the mixture of *P. gingivalis* and *T. denticola* cultures were prepared with *P. gingivalis* $\text{OD}_{600} = 0.05$ in BHI and *T. denticola* $\text{OD}_{600} = 0.05$ in NOS at 37°C under anaerobic conditions. After incubations of 48 h with each species, medium was removed and samples were washed with phosphate-buffered saline (PBS, Biochrom GmbH, Berlin, Germany). Samples were fluorescence stained with LIVE/DEAD BacLight Bacterial Viability Kit (Life Technologies, Darmstadt, Germany) at 1:1000 in PBS for 15 min at room temperature according to the manufacturer's protocol. Stained biofilms were fixed with 2.5% glutaraldehyde (Carl Roth GmbH + Co. KG, Karlsruhe, Germany) for 15 min at 4°C . The two fluorescent dyes Syto9 and propidium iodide were excited at 488 and 552 nm, and emission was detected at 500–552 nm and 600–700 nm, respectively. All samples were imaged by confocal laser-scanning microscopy (CLSM, Leica TCS SP2, Leica Microsystems, Mannheim, Germany). Acquired images were further processed with the Imaris (8.2) software package (Bitplane AG, Zurich, Switzerland).

Biofilm Cultivation in a Flow Chamber System: Biofilm formation assays under flow conditions were performed in a previously developed flow chamber system containing brain heart infusion media supplemented with 5% sucrose (Carl Roth GmbH + Co. KG) and $10\ \mu\text{L mL}^{-1}$ vitamin K.^[35] Multispecies biofilms were cultured on coated and uncoated titanium discs using the Hanoverian oral multispecies biofilm implant flow chamber (HOBIC) model.^[48] In brief, *S. oralis*, *A. naeslundii*, *V. dispar*, and *P. gingivalis* were grown for 18 h at 37°C as individual cultures in BHI/vitamin K under anaerobic conditions (80% N_2 , 10% H_2 , and 10% CO_2) and adjusted to an optical density (OD_{600}) of 0.5. Equal volumes from each of the indicated bacteria were mixed and added to a bioreactor containing 1.8 L BHI/vitamin K at a dilution of 1: 45. Multispecies biofilms were grown for 24 h at a flow rate of $100\ \mu\text{L min}^{-1}$ before being stained using the LIVE/DEAD BacLight Bacterial Viability Kit as described previously.^[48] Biofilms were imaged using CLSM and analyzed with the Imaris (8.2) software package as described above ($N = 9$, 5 images per sample and in total 45 images per surface).

Fluorescence In Situ Hybridization (FISH): After incubation of *S. o.*-coated or uncoated titanium with multispecies bacteria in the flow

chamber system, specimens were fixed with 50% ethanol for 40 min at a flow rate of 150 $\mu\text{L min}^{-1}$. The samples were subjected to fluorescence in situ hybridization according to a protocol established previously.^[49] Briefly, samples were first made permeable with 1 $\mu\text{g mL}^{-1}$ lysozyme for 30 min at 46 °C, then hybridized with 8×10^{-6} M of each 16S rRNA probe in urea-NaCl buffer (Table S1, Supporting Information). Stained implants were merged in PBS and imaged by CLSM with PMT detectors. The first sequence was detected with ALEXA Fluor405 using 405 nm laser at an emission range of 413–477 nm and ALEXA Fluor568 signals with 552 nm laser at an emission range of 576–648 nm. The second sequence was detected with ALEXA Fluor488 signals with the 488 nm laser at the emission range of 509–576 nm together with ALEXA Fluor647 signals using 638 nm laser and an emission range of 648–777 nm. Image adjustments were performed with Imaris (8.2) software package.

Scanning Electron Microscopy (SEM) Analysis: Samples exposed to biofilms were additionally observed using an electron microscope ($N = 6$). After 48 h of incubation with bacterial cultures, the bacterial medium was removed and *S. o.*-coated and uncoated titanium were washed twice with PBS, fixed in 2.5% glutaraldehyde for 30 min and washed again with PBS. Samples were dehydrated in ascending series (25%, 50%, 75%, 90%, and 100%) of ethanol (J. T. Baker, Phillipsburg, New Jersey, USA) for 5 min in each concentration. Dehydrated samples were treated in a Blazer CPD 030 Critical Point Dryer (BAL-TECH; Balzers, Liechtenstein) and then sputter coated with gold in an E5400 SEM Coating System (Polaron, Watford, United Kingdom). Scanning electron microscopy was performed with a SEM 505 microscope (Philips, Eindhoven, Netherlands). SEM images were processed with a custom build SEM Software 4.5.^[50]

Bacterial Single Cell Adhesion Force Spectroscopy: Adhesive forces of *S. oralis* or *P. gingivalis* on *S. o.*-coated or uncoated titanium were measured with a FlexFPM atomic force microscope (Nanosurf AG, Liestal, Switzerland) connected to a FluidFM pressure control system (Cytosurge AG, Zürich, Switzerland) mounted on an inverted microscope (Lclipse Ti-S, Nikon GmbH, Düsseldorf, Germany), according to a previously described protocol.^[51] Briefly, silicon cantilevers with a circular 300 nm opening and a theoretical spring constant of 0.6 N m^{-1} (FluidFM Nanopipette, Cytosurge AG) were used. Before measurements, cantilevers were filled with degassed and filtered phosphate-buffered saline (PBS) and their sensitivity was measured. *S. o.*-coated or uncoated titanium samples were inserted in a 1 mm glass ring placed in 50 mm glass dish (WillCo Wells B. V., Amsterdam, The Netherlands). Freshly cultivated *S. oralis* or *P. gingivalis* were diluted in filtered phosphate-buffered saline to a final optical density (OD_{600}) of 0.005 (approximately 1×10^6 CFU mL^{-1}) and then added into glass dishes. Bacterial cells were captured with the cantilever for 5 s with 400 mbar of negative pressure and then transferred onto the specimen to measure single bacterial single cell adhesion force spectroscopy. Bacteria were allowed to interact with the surface for 5 s with contact force of 0.75 nN and enabled with force feedback and then retracted with a velocity of 1 $\mu\text{m s}^{-1}$. Each of the coated or plain titanium surfaces was subjected to 12 measurements with individual bacterial cells, each at 16 different positions in total 192 force–distance curves. From the resulting force–distance curves, maximum adhesion force was calculated with program AtomicJ.^[52] Data visualization and statistical analysis were performed with GraphPad Prism software 8.0 (GraphPad Prism Software Inc., La Jolla, USA).

In Vitro Mammalian Cell Culture Assay: The cell toxicity assay was performed with human gingival fibroblasts (HGFs) by a fluorometric CellTiter-Blue assay, which measures cellular reduction capacity through resazurin color change.^[26] Human gingival fibroblasts were cultured in Dulbecco's modified Eagle medium (Biochrom AG, Berlin, Germany), supplemented with 10% fetal bovine serum (PAN-BIOTECH GmbH, Aidenbach, Germany), 100 U mL^{-1} penicillin, and 100 $\mu\text{g mL}^{-1}$ streptomycin (Biochrom AG, Berlin, Germany) in a humidified cell culture incubator at 37 °C in the presence of 5% CO_2 . Fibroblasts were seeded on *S. o.*-coated or uncoated titanium with a cell density of 1×10^5 cells per disc. At 24, 48, and 72 h after incubation, medium from cells was replaced with CellTiter-Blue reagent (Promega, Mannheim, Germany) and incubated for 4 h at

37 °C. CellTiter-Blue reagent was collected from the respective cells and its fluorescence was measured by a multiwell plate reader ($\lambda_{\text{ex}} = 530$ nm, $\lambda_{\text{em}} = 590$ nm, Synergy 2, BioTek). Relative fluorescence units (RFU) were measured by the multifunctional microplate reader Tecan Infinite 200 PRO (IBL International, GmbH, Hamburg, Germany). For direct monitoring of cellular attachment and morphology, human gingival fibroblasts were seeded on uncoated and coated implant surfaces at a density of 1×10^5 cells per ml in Dulbecco's modified Eagle medium (Biochrom AG, Berlin, Germany), supplemented with 10% fetal bovine serum (PAN-BIOTECH GmbH, Aidenbach, Germany), 100 U mL^{-1} penicillin, and 100 $\mu\text{g mL}^{-1}$ streptomycin (Biochrom AG, Berlin, Germany) ($N = 8$ per group). The cultured cells were incubated for 72 h at 37 °C in 5% CO_2 . The loosely adherent cells were removed from the implant surfaces by washing twice with phosphate-buffered saline (PBS). Cells in experiment wells were stained with LIVE/DEAD BacLight for 30 minutes. Stained cells were fixed with 1.5% glutaraldehyde and imaged with confocal laser scanning microscopy.

Supporting Information

Supporting Information is available from the Wiley Online Library or from the author.

Acknowledgements

The authors acknowledge the excellent support of Marly Dalton for scanning electron microscopy, Nadine Kommerein for the multispecies biofilm model in the flow chamber and Jörn Schaeske for the cell culture assay. M.I.R. was supported by the Alexander von Humboldt Foundation. This research project was supported by the BIOFABRICATION FOR NIFE Initiative. NIFE is the Lower Saxony Center for Biomedical Engineering, Implant Research and Development, a joint translational research center of the Hannover Medical School, the Leibniz University Hannover, the University of Veterinary Medicine Hannover and the Laser Zentrum Hannover e. V., The BIOFABRICATION FOR NIFE Initiative was financially supported by the ministry of Lower Saxony and the VolkswagenStiftung (both BIOFABRICATION FOR NIFE: VWZN2860). The authors acknowledge the help of BioRender.com in facilitating the generation of schematic diagrams.

Open access funding enabled and organized by Projekt DEAL.

Conflict of Interest

Muhammad Imran Rahim has patent #EP3741398 (A1) — 2020-11-25 pending to European Patent Office. Meike Stiesch, Michael Eisenburger, Nico S. Stumpp has patent #EP3741398 (A1) — 2020-11-25 pending to European Patent Office. Muhammad Imran Rahim has patent #WO-2020234332-A1 pending to Patent Cooperation Treaty (PCT). Meike Stiesch, Michael Eisenburger, Nico S. Stumpp has patent #WO-2020234332-A1 pending to WO-2020234332-A1. There are no other activities.

Data Availability Statement

Research data are not shared.

Keywords

biomaterial-associated infections, commensal bacteria, implant surface coating, periodontal pathogens, *Streptococcus oralis*

Received: September 10, 2021

Revised: October 3, 2021

Published online: November 10, 2021

- [1] a) M.-N. Abdallah, Z. Badran, O. Ciobanu, N. Hamdan, F. Tamimi, *Adv. Healthcare Mater.* **2017**, *6*, 1700549; b) A. L. Palkowitz, T. Tuna, S. Bishti, F. Böke, N. Steinke, G. Müller-Newen, S. Wolfart, H. Fischer, *Adv. Healthcare Mater.* **2021**, *10*, 2100132.
- [2] a) W. Heuer, A. Kettenring, S. N. Stumpp, J. Eberhard, E. Gellermann, A. Winkel, M. Stiesch, *Clin. Oral Invest.* **2012**, *16*, 843; b) B. Grössner-Schreiber, M. Griepentrog, I. Haustein, W. D. Müller, K. P. Lange, H. Briedigkeit, U. B. Göbel, *Clin. Oral Implants Res.* **2001**, *12*, 543.
- [3] E. O’Cearbhaill, *Sci. Transl. Med.* **2019**, *11*, eaaz3709.
- [4] a) H. Dreyer, J. Grischke, C. Tiede, J. Eberhard, A. Schweitzer, S. E. Toikkanen, S. Glöckner, G. Krause, M. Stiesch, *J. Periodontol Res.* **2018**, *53*, 657; b) F. Schwarz, J. Derks, A. Monje, H. L. Wang, *J. Clin. Periodontol.* **2018**, *45*, S246.
- [5] J. H. Fu, H. L. Wang, *Periodontology* **2020**, *84*, 145.
- [6] a) H.-C. Flemming, J. Wingender, *Nat. Rev. Microbiol.* **2010**, *8*, 623; b) M. I. Rahim, S. P. Szafranski, A. Ingendoh-Tsakmakidis, M. Stiesch, P. P. Mueller, *Colloids Surf., B* **2020**, *186*, 110684.
- [7] T. Bjarnsholt, O. Ciofu, S. Molin, M. Givskov, N. Høiby, *Nat. Rev. Drug Discovery* **2013**, *12*, 791.
- [8] T. Wei, Q. Yu, H. Chen, *Adv. Healthcare Mater.* **2019**, *8*, 1801381.
- [9] M. Lipsitch, *Trends Microbiol.* **2001**, *9*, 438.
- [10] L. Czaplewski, R. Bax, M. Clokie, M. Dawson, H. Fairhead, V. A. Fischetti, S. Foster, B. F. Gilmore, R. E. W. Hancock, D. Harper, I. R. Henderson, K. Hilpert, B. V. Jones, A. Kadioglu, D. Knowles, S. Ólafsdóttir, D. Payne, S. Projan, S. Shaunak, J. Silverman, C. M. Thomas, T. J. Trust, P. Warn, J. H. Rex, *Lancet Infect. Dis.* **2016**, *16*, 239.
- [11] a) D. R. Monteiro, L. F. Gorup, A. S. Takamiya, A. C. Ruvollo-Filho, E. R. d. Camargo, D. B. Barbosa, *Int. J. Antimicrob. Agents* **2009**, *34*, 103; b) M. Salwiczek, Y. Qu, J. Gardiner, R. A. Strugnell, T. Lithgow, K. M. McLean, H. Thissen, *Trends Biotechnol.* **2014**, *32*, 82; c) B. R. Coad, H. J. Griesser, A. Y. Peleg, A. Traven, *PLoS Pathog.* **2016**, *12*, e1005598.
- [12] P. Makvandi, C.-y. Wang, E. N. Zare, A. Borzacchiello, L.-n. Niu, F. R. Tay, *Adv. Funct. Mater.* **2020**, *30*, 1910021.
- [13] a) I. Banerjee, R. C. Pangule, R. S. Kane, *Adv. Mater.* **2011**, *23*, 690; b) S. Wu, J. Xu, L. Zou, S. Luo, R. Yao, B. Zheng, G. Liang, D. Wu, Y. Li, *Nat. Commun.* **2021**, *12*, 3303.
- [14] J. Buxadera-Palomero, C. Canal, S. Torrent-Camarero, B. Garrido, F. Javier Gil, D. Rodríguez, *Biointerphases* **2015**, *10*, 029505.
- [15] E. Ostuni, R. G. Chapman, M. N. Liang, G. Meluleni, G. Pier, D. E. Ingber, G. M. Whitesides, *Langmuir* **2001**, *17*, 6336.
- [16] G. Cheng, H. Xue, Z. Zhang, S. Chen, S. Jiang, *Angew. Chem., Int. Ed.* **2008**, *47*, 8831.
- [17] K. Knop, R. Hoogenboom, D. Fischer, U. S. Schubert, *Angew. Chem., Int. Ed.* **2010**, *49*, 6288.
- [18] S. Guglielmetti, V. Taverniti, M. Minuzzo, S. Arioli, M. Stuknyte, M. Karp, D. Mora, *Appl. Environ. Microbiol.* **2010**, *76*, 3948.
- [19] I. Laleman, E. Yilmaz, O. Ozcelik, C. Haytac, M. Pauwels, E. R. Herrero, V. Slomka, M. Quirynen, B. Alkaya, W. Teughels, *J. Clin. Periodontol.* **2015**, *42*, 1032.
- [20] a) L. Näse, K. Hatakka, E. Savilahti, M. Saxelin, A. Pönkä, T. Poussa, R. Korpela, J. H. Meurman, *Caries Res.* **2001**, *35*, 412; b) A. Ahola, H. Yli-Knuuttila, T. Suomalainen, T. Poussa, A. Ahlström, J. H. Meurman, R. Korpela, *Arch. Oral Biol.* **2002**, *47*, 799; c) E. Caglar, S. Kavaloglu Cildir, S. Ergeneli, N. Sandalli, S. Twetman, *Acta Odontol. Scand.* **2006**, *64*, 314; d) E. Caglar, S. Kavaloglu, O. Kuscü, N. Sandalli, P. Holgerson, S. Twetman, *Clin. Oral Invest.* **2007**, *11*, 425; e) S. K. Cildir, D. Germec, N. Sandalli, F. I. Ozdemir, T. Arun, S. Twetman, E. Caglar, *Eur. J. Orthod.* **2009**, *31*, 407.
- [21] a) P. A. Wescombe, N. C. K. Heng, J. P. Burton, C. N. Chilcott, J. R. Tagg, *Future Microbiol.* **2009**, *4*, 819; b) J. P. Burton, B. K. Drummond, C. N. Chilcott, J. R. Tagg, W. M. Thomson, J. D. F. Hale, P. A. Wescombe, *J. Med. Microbiol.* **2013**, *62*, 875.
- [22] E. Çağlar, N. Sandalli, S. Twetman, S. Kavaloglu, S. Ergeneli, S. Selvi, *Acta Odontol. Scand.* **2005**, *63*, 317.
- [23] A. Mahdhi, N. Leban, I. Chakroun, M. A. Chaouch, J. Hafsa, K. Fdhila, K. Mahdouani, H. Majdoub, *Microb. Pathog.* **2017**, *109*, 214.
- [24] E. Ciandrini, R. Campana, W. Baffone, *Arch. Oral Biol.* **2017**, *78*, 48.
- [25] L. Tan, J. Fu, F. Feng, X. Liu, Z. Cui, B. Li, Y. Han, Y. Zheng, K. W. K. Yeung, Z. Li, S. Zhu, Y. Liang, X. Feng, X. Wang, S. Wu, *Sci. Adv.* **2020**, *6*, abab5723.
- [26] K. Doll, E. Fadeeva, J. Schaeske, T. Ehmke, A. Winkel, A. Heisterkamp, B. N. Chichkov, M. Stiesch, N. S. Stumpp, *ACS Appl. Mater. Interfaces* **2017**, *9*, 9359.
- [27] T. F. Moriarty, R. Kuehl, T. Coenye, W.-J. Metsemakers, M. Morgenstern, E. M. Schwarz, M. Riool, S. A. J. Zaat, N. Khana, S. L. Kates, R. G. Richards, *EFORT Open Rev.* **2017**, *1*, 89.
- [28] Y. Wang, G. Subbiahdoss, J. Swartjes, H. C. van der Mei, H. J. Busscher, M. Libera, *Adv. Funct. Mater.* **2011**, *21*, 3916.
- [29] F. E. Dewhirst, T. Chen, J. Izard, B. J. Paster, A. C. R. Tanner, W.-H. Yu, A. Lakshmanan, W. G. Wade, *J. Bacteriol.* **2010**, *192*, 5002.
- [30] a) L. V. Hooper, J. I. Gordon, *Science* **2001**, *292*, 1115; b) H. Tlaskalová-Hogenová, R. Štěpánková, T. Hudcovic, L. Tučková, B. Cukrowska, R. Lodinová-Žádníková, H. Kozáková, P. Rossmann, J. Bártová, D. Sokol, D. P. Funda, D. Borovská, Z. Řeháková, J. Šinkora, J. Hofman, P. Drastich, A. Kokešová, *Immunol. Lett.* **2004**, *93*, 97.
- [31] a) P. I. Diaz, N. I. Chalmers, A. H. Rickard, C. Kong, C. L. Milburn, R. J. Palmer Jr., P. E. Kolenbrander, *Appl. Environ. Microbiol.* **2006**, *72*, 2837; b) P. I. Diaz, Z. Xie, T. Sobue, A. Thompson, B. Biyikoglu, A. Ricker, L. Ikononou, A. Dongari-Bagtzoglou, *Infect. Immun.* **2012**, *80*, 620.
- [32] A. Ingendoh-Tsakmakidis, J. Eberhard, C. S. Falk, M. Stiesch, A. Winkel, *Cells* **2020**, *9*, 1226.
- [33] M. Bek-Thomsen, H. Tettelin, I. Hance, K. E. Nelson, M. Kilian, *Infect. Immun.* **2008**, *76*, 1889.
- [34] R. Mohanty, S. J. Asopa, M. D. Joseph, B. Singh, J. P. Rajguru, K. Saidath, U. Sharma, *J. Family Med. Primary Care* **2019**, *8*, 3480.
- [35] H. Rath, S. N. Stumpp, M. Stiesch, *PLoS One* **2017**, *12*, e0172095.
- [36] a) S. E. A. Camargo, X. Xia, C. Fares, F. Ren, S.-M. Hsu, D. Budei, C. Aravindrajha, L. Kesavalu, J. F. Esquivel-Upshaw, *Materials* **2021**, *14*, 4357; b) V. Meyer-Kobbe, K. Doll, M. Stiesch, R. Schwestka-Polly, A. Demling, *J. Orofacial Orthop.* **2018**, *80*, 32.
- [37] Q. Q. Qiu, W. Sun, J. Connor, *Compr. Biomater.* **2011**, *4*, 127.
- [38] G. Kaci, D. Goudercourt, V. Dennin, B. Pot, J. Doré, S. D. Ehrlich, P. Renault, H. M. Blottière, C. Daniel, C. Delorme, *Appl. Environ. Microbiol.* **2014**, *80*, 928.
- [39] S. E. A. Camargo, T. Roy, X. Xia, C. Fares, S.-M. Hsu, F. Ren, A. E. Clark, D. Neal, J. F. Esquivel-Upshaw, *Materials* **2021**, *14*, 342.
- [40] I. La Mantia, A. Varricchio, G. Ciprandi, *Int. J. Gen. Med.* **2017**, *10*, 171.
- [41] L. Mei, Y. Ren, H. J. Busscher, Y. Chen, H. C. van der Mei, *J. Dent. Res.* **2009**, *88*, 841.
- [42] X. Sheng, Y. P. Ting, S. O. Pehkonen, *J. Colloid Interface Sci.* **2008**, *321*, 256.
- [43] P. Ahangar, S. J. Mills, L. E. Smith, S. Gronthos, A. J. Cowin, *npj Regener. Med.* **2020**, *5*, 24.
- [44] a) T. Ara, K. Kurata, K. Hirai, T. Uchihashi, T. Uematsu, Y. Imamura, K. Furusawa, S. Kurihara, P. L. Wang, *J. Periodontol Res.* **2009**, *44*, 21; b) R. Cheng, D. Choudhury, C. Liu, S. Billet, T. Hu, N. A. Bhowmick, *Cell Death Discovery* **2015**, *1*, 15046.
- [45] B. Kinikoglu, O. Damour, V. Hasirci, *J. Artif. Organs* **2015**, *18*, 8.
- [46] D. Buser, L. Sennerby, H. De Bruyn, *Periodontology* **2017**, *73*, 7.

- [47] J. C. Fenno, *Curr. Protoc. Microbiol.* **2005**, 12, 12B.1.
- [48] N. Kommerein, K. Doll, N. S. Stumpp, M. Stiesch, *PLoS One* **2018**, 13, e0196967.
- [49] N. Kommerein, S. N. Stumpp, M. Müsken, N. Ehlert, A. Winkel, S. Häußler, P. Behrens, F. F. R. Buettner, M. Stiesch, *PLoS One* **2017**, 12, e0173973.
- [50] Gebert, Preiss, J. *Microsc.* **1998**, 191, 297.
- [51] K. Doll, I. Yang, E. Fadeeva, N. Kommerein, S. P. Szafranski, G. Bei der Wieden, A. Greuling, A. Winkel, B. N. Chichkov, N. S. Stumpp, M. Stiesch, *ACS Appl. Mater. Interfaces* **2019**, 11, 23026.
- [52] P. Hermanowicz, M. Sarna, K. Burda, H. Gabryś, *Rev. Sci. Instrum.* **2014**, 85, 063703.